Minimum Fluidization Velocity of a Three-Phase Conical Fluidized Bed in Comparison to a Cylindrical Fluidized Bed

ARTICLE *in* INDUSTRIAL & ENGINEERING CHEMISTRY RESEARCH · JUNE 2008

Impact Factor: 2.59 · DOI: 10.1021/ie8001974

4 AUTHORS, INCLUDING:

Dandan Zhou
Jilin University
39 PUBLICATIONS **137** CITATIONS
SEE PROFILE

Shuangshi Dong
Jilin University
33 PUBLICATIONS **125** CITATIONS
SEE PROFILE

Xiaotao Tony Bi
University of British Columbia - Vancouver
141 PUBLICATIONS **1,532** CITATIONS
SEE PROFILE

Minimum Fluidization Velocity of a Three-Phase Conical Fluidized Bed in Comparison to a Cylindrical Fluidized Bed

Dandan Zhou,[†,‡] Shuangshi Dong,[§] Heli Wang,[†] and Hsiaotao T. Bi*[,⊥]

School of Water Resources and Environmental Science, China University of Geosciences (Beijing), Beijing, China, School of Municipal and Environmental Engineering, Harbin Institute of Technology, Harbin, China, and Department of Chemical and Biological Engineering, University of British Columbia, Vancouver, Canada

Hydrodynamic characteristics of a gas−liquid−solid conical fluidized bed were studied and compared with both liquid−solid conical beds and three-phase cylindrical fluidized beds. The effect of bubbles on particle mixing, pressure drop, and minimum fluidization velocity were discussed. Minimum fluidization velocities predicted by modified Ergun equation which accounts for the variation of the cross-sectional area with the bed height were found to be in good agreement with the liquid−solid conical fluidized bed data. The models of Song et al. [*Can. J. Chem. Eng.* 1989, *67*, 265] and Zhang et al. [*Power Tech.* 1998, *100*, 113; PhD. Thesis, 1996], derived originally for three-phase cylindrical fluidized beds, respectively, were modified for the prediction of U_{mf} in a three-phase conical fluidized bed by accounting for the geometrical variation of the conical bed. It is found that the modified Song et al. model gave a better agreement than the modified Zhang et al. model in comparison with the current experimental data. However, the prediction of the modified Zhang et al. model is much improved when the parameter α, fractional gas holdup, was estimated using the equation from the Song et al. model.

Introduction

Fluidized beds as chemical reactors offer many unique advantages such as large interfacial surface areas between the fluid (gas or liquid) and particles, high fluid−particle contact efficiency, excellent heat transfer, uniform bed temperature, and the ability to handle a wide range of types of particles and a large quantity of particulate materials.[1–4] Fluidized-bed reactors include gas−solid, liquid−solid, and gas−liquid−solid fluidized-bed reactors in terms of the fluid−particulate systems.[5] Gas−liquid−solid fluidization has already been applied in many biochemical reactors and in chemical processes where solid particles need to be contacted with both liquid and gas, for example, aerobic wastewater treatment bioreactors,[6,7] sewage sludge pyrolysis[8] and catalyzed reaction systems,[9] etc.

Fluidized beds can also be classified into cylindrical bed and conical (tapered) bed in terms of the reactor shape. Cylindrical bed is the major type of laboratory and commercial reactors. However, conical beds have been applied widely in various processes, such as the coating, drying and granulation of particulate materials and immobilized wastewater treatment and microorganism processes. In a conical bed, where the cross section increases with the bed height, higher velocity is maintained at the lower part of the column, making it possible to fluidize particles of wide size distributions. Toyohara and Kawamura showed that particles in a tapered gas−solids fluidized bed circulated between core and the annulus region in an almost perfectly mixed state, which helped promote mixing.[10] Webster showed that axial liquid mixing increased in the tapered liquid−solids fluidized beds even for a small taper angle (0.5°), in comparison with the cylindrical bed.[11] The downward flow and channeling of liquid, however, only occurred in conical beds using small size particles.

* To whom correspondence should be addressed. E-mail: xbi@chml.ubc.ca. Tel.: 604-822-4408. Fax: 604-822-6003.

[†] China University of Geosciences (Beijing).

[‡] Present address: College of Environment and Resources, Jilin University, Changchun 130021, China.

[§] Harbin Institute of Technology.

[⊥] University of British Columbia.

Conical fluidized-bed reactors have their unique advantages over cylindrical ones in some applications. For an immobilized water treatment bioreactor, both the superficial velocity and drag force of the fluid exerted on the bioparticles in the upper part of the conical fluidized-bed bioreactor will be smaller than the cylindrical bed. As a result, bioparticles will be prevented from being carried out from the top of the reactor and the operating range of the flow rate of conical bioreactors can be broadened.[12]

Due to its distinct geometry, a conical fluidized bed possesses quite different hydrodynamic characteristics compared to conventional cylindrical beds. In both gas−solid and liquid−solid tapered beds, at least four flow regimes have been identified, ranging from fixed beds, partially fluidized beds, fully fluidized beds, to turbulent fluidized beds.[10,13–15] At a low fluid flow rate, the fluid passes upward through the bed without disturbing the particles and the pressure drop ($-\Delta P_T$) increases steadily with the increase in the flow rate. The lower region of the bed becomes partially fluidized when the maximum pressure drop is reached, when a cavity starts to appear right above the distributor, containing a relatively small number of particles. The superficial fluid velocity based on the column inlet diameter at this point is defined as the minimum velocity of partial fluidization. Particles move freely in the fluidized region where the voidage is greater than that in the surrounding fixed bed region. In this partially fluidized regime, the net pressure drop decreases with the flow rate. Full fluidization is reached when the upper surface layer of the bed reaches the fluidization state. In the fully fluidized bed, particles in the center region move upward and particles move downward in the core region at a lower speed. As the flow rate further increases in the fully fluidized regime, the interface between the core and the annulus disappears gradually, with particles moving more randomly, representing a turbulently fluidized regime.

Several studies have attempted to predict the minimum fluidization velocity of both gas−solid and liquid−solid tapered fluidized beds by incorporating the conical geometry into the minimum fluidization velocity equation, which was originally derived for cylindrical fluidized beds. [10,14–18] However, little

10.1021/ie8001974 CCC: $40.75
Published on Web 06/25/2008

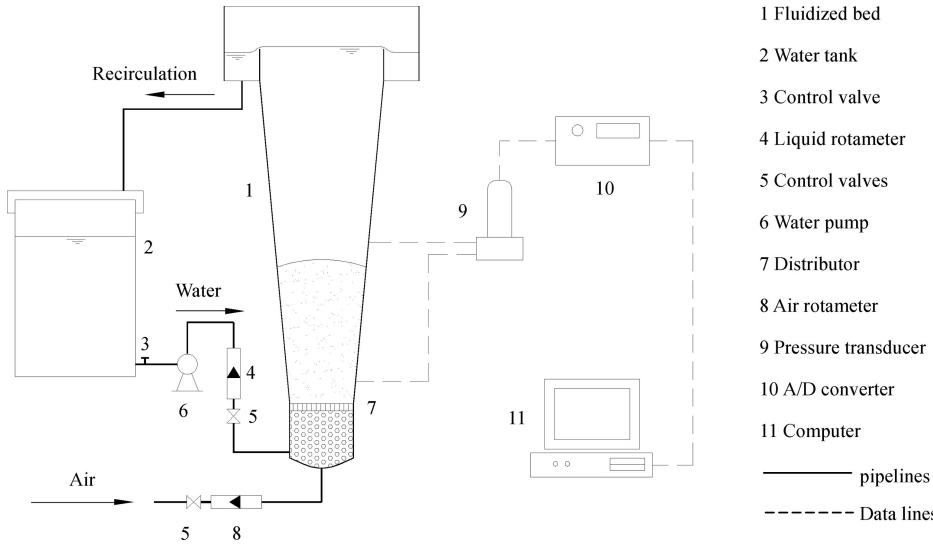

Figure 1. Experimental setup.

Table 1. Physical Properties of Particles

	d_p mm	ρ_s kg/m^3	ε_0	Φs
activated carbon	0.64	1317	0.388	1.0
glass beads	0.62	2490	0.387	1.0
glass beads	0.98	2490	0.391	1.0

work has been done on the gas−liquid−solid three-phase tapered beds. The objective of this research was to study the hydrodynamic characteristics of a conical fluidized bed operated with both liquid and gas−liquid as the fluidizing medium.

Experimental Apparatus and Procedures

Experimental Apparatus. One cylindrical column and one conical column with a tapered angle of 8° were used in this research, with the experimental setup shown in Figure 1. Both units consist of four Plexiglas sections: a 200 mm high plenum chamber packed with 2.5 mm plastic beads for improving the fluid distribution, a distributor plate with 2% opening ratio appropriate number of 1.6 mm holes above the plenum chamber, a test section, and an expanded section on the top. The test section of the cylindrical bed is 762 mm tall and 102 mm in inner diameter. The test section of conical bed is 435 mm high with a diameter of 89 mm at the bottom and 203 mm at the top. A screen was installed on top of the distributor plate to prevent particles from falling into the plenum chamber. The gas−liquid flow is cocurrent and upward in this study, with the flow rates of both gas and liquid being measured by precalibrated rotameters and controlled by valves, respectively. Three types of spherical particles were used in this research, with their physical properties summarized in Table 1. The diameter of glass beads and activated carbon was determined by averaging the diameters measured for about 100 individual particles with a micrometer. The density of the glass beads was measured using the water displacement method in which the packing voidage was obtained by displaced water volume when the particles were placed into a graduated cylinder filled with water. For porous activated carbon particles, the wet particle density is an important parameter, since water will penetrate into micropores of the porous particles in the liquid−solid fluidized bed. By assuming that the inner pores of the particle will be fully occupied by water, the wet density of porous particles can be calculated from the following equation

$$\rho_w = \rho_r(1-\varepsilon_p) + \rho_l\varepsilon_p \tag{1}$$

where ρ_w is the wet density of the porous particle, ρ_r is the skeleton density, ρ_l is liquid density, and ε_p is the porosity of the particle. The skeleton density of particles, ρ_r, was obtained by dividing the weight of given amount of dry particles by the volume of the particles excluding the inner pores obtained from the water displacement method. The dry particles were placed into a graduated cylinder originally filled up with a given volume of water. To eliminate air bubbles potentially trapped in the pores of the particles, the cylinder was agitated frequently after particles were added and was left for 24 h before the final volume was measured. The volume of the particles excluding the inner pores was taken as the difference between the final volume and the original volume of the cylinder by assuming that water fully penetrated into all inner pores.

The term ε_p, the porosity of particles, was obtained by the following equation,

$$\varepsilon_p = 1 - \frac{\rho_s}{\rho_r} \tag{2}$$

with the particle density ρ_s obtained from

$$\rho_s = \frac{W}{\frac{1}{4}\pi d_p^{\,2} n} \tag{3}$$

where W is the weight of given number of dry particles, d_p is the average particle diameter which was determined by micrometer as mentioned above, and n is the given number of particles. A total of 500−800 particles were counted in each test over 3−4 repeats for a high accuracy.

The bed temperature was maintained at room temperature, 22 ± 1 °C in all experiments.

Experimental Procedure. The minimum fluidizing velocity was obtained from the pressure drop versus the liquid velocity curve, with the pressure drop measured between two ports using a differential pressure transducer (Omega Model PX-750) and recorded by a computer via an analog/digital (A/D) interface card. One of the two ports was located right above the distributor, and the other was installed right above the expanded bed surface. The pressure transducer was precalibrated with the use of a manometer. Figure 3 is a sample pressure drop versus superficial velocity plot illustrating how to obtain the minimum fluidization velocity in both two-phase and three-phase fluidized beds. For each run, the flow rate of water was increased

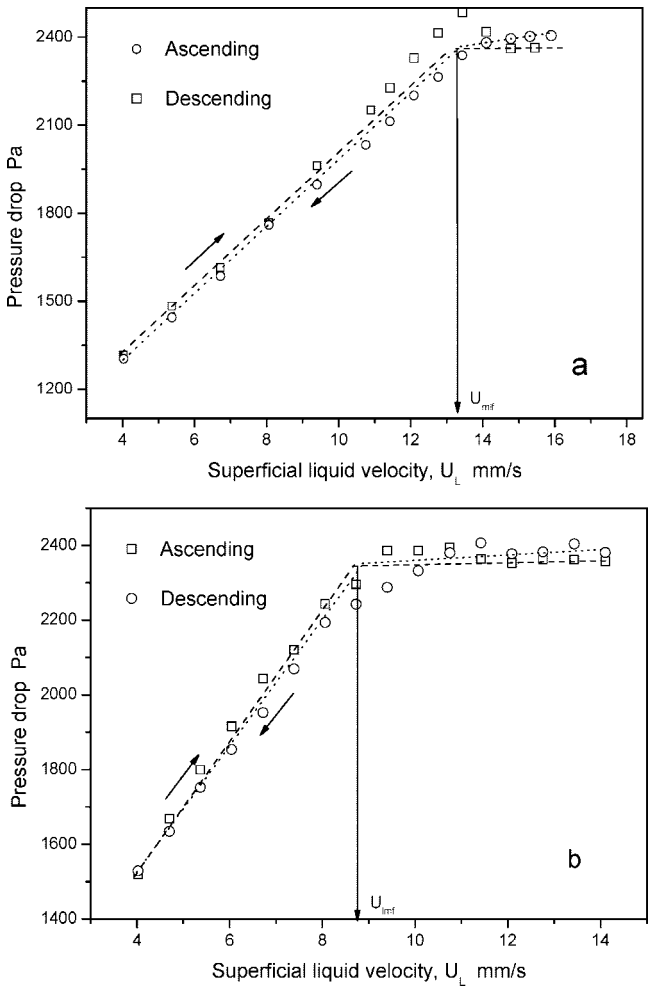

Figure 2. Pressure drop as a function of superficial liquid velocity at the inlet of (a) liquid−solid and (b) gas−liquid−solid conical fluidized beds: 0.98 mm GB, 190 mm packed bed height.

gradually by adjusting the control valve carefully at first (flow ascending process), followed by the gradual decrease (descending process) after the bed was fully fluidized and the pressure drop leveled off. Here, 1200 data points were collected at each velocity for the determination of the average pressure drop.

Experimental Results

Flow Regimes of Three-Phase Conical Beds. One of the unique phenomena of conical fluidized beds is the partial fluidization state. The decreasing superficial fluid velocity along the elevation results in the reduction of drag force exerted on particles at an upward axial direction of the reactor. As a result, the lower part of the bed is fluidized first when the upper part still remains at the static state over a range of superficial fluid velocities before the entire bed is fluidized.

The flow pattern in liquid−solid (L-S) and gas−liquid−solid (G-L-S) conical fluidized beds with 0.6 mm glass beads was observed carefully from the Plexiglass wall of the column at superficial liquid velocities of 3.9, 4.4, 6.0, and 7.7 mm/s. Internal jetting or streaming occurred in the L-S conical bed and became more obvious as the superficial liquid velocity increased. A higher liquid velocity at the lower part exerts a higher drag force on particles in the bottom region. The high drag force, combined with the compaction from the upper packed particles, may be responsible for creating such an imperfect flow pattern, i.e. channeling or streaming, in the lower part of the bed. Most of the particles maintained an upward flow in the center region and a downward flow in the annulus region except those particles in the channeling stream where they flowed randomly at a much higher speed. A similar phenomenon was reported in the previous study of Webster and Perona[11] who found that channeling only occurred in a tapered bed within a certain range of Reynolds number in some specific region of the column.

The flow distribution appeared to be improved after gas bubbles were introduced into the column in the three-phase system. Channeling or streaming became much smaller than the liquid−solid conical bed at the same superficial liquid velocity. The drag force in a gas−liquid−solid conical fluidized bed is induced by both liquid and gas bubbles. The upward flow of bubbles tends to exert more shear force to the packed particles in the upper region of the column, loosening particles to reduce the lateral nonuniformity of the shear stress. As a result, the nonuniform distribution of liquid flow is reduced. When the gas velocity was increased from 0.6 to 1.2 mm/s, it was found that channeling disappeared completely because of the agitation of more energetic bubbles at a higher gas velocity. On the other hand, the difference of bubbling intensity also contributed to the particles upward flow in the core region and downward flow in the annulus region.

Pressure Drop of Three-Phase Conical Beds. Total pressure drop in fluidized beds can be expressed as the sum of hydrostatic and frictional terms. The total pressure drop in a G-L-S fluidized bed can be expressed as

$$\Delta P_T = (1-\varepsilon_g)\rho_l g h + \varepsilon_g h + \Delta P_F \quad (4)$$

The last term, pressure drop due to frictional force, is a function of the fluid velocity, which will be discussed in more detail later. Since the local fluidizing velocity varies along the axial direction in the conical bed, the hydrodynamic model expressions derived for cylindrical beds cannot be directly applied to conical beds.

Figures 2 and 3 show the total pressure drop as a function of the superficial liquid velocity at the bottom of the conical and cylindrical beds, respectively, with an initial bed height of 190 mm. The pressure drop curves of the conical bed and cylindrical bed are seen to be quite different. For a liquid−solid conical fluidized bed (Figure 2A), the pressure drop magnitude increases steadily at first with increasing the superficial velocity until a maximum value is reached, followed by a sudden drop before reaches almost a constant value. For the liquid−solid cylindrical fluidized bed (Figure 3A), there is no obvious decrease after the steady increase of the pressure drop. Furthermore, the maximum pressure drop (P_{MAX}), which is considered to correspond to the critical superficial velocity or the partial fluidization velocity, in the conical bed is greater than that in the cylindrical bed. The minimum fluidization velocity of conical bed is also seen to be greater than the cylindrical bed. In a conical bed, the decreasing fluidizing velocity with the bed height is accompanied with decreased drag forces on particles. A higher velocity in the bed entrance is thus needed to fluidize particles at the upper region of the conical bed. In the fluid velocity descending process, the pressure drop decreased steadily, with no peak encountered. Such a trend is identical to those observed by previous researchers (e.g., Peng and Fan[13]).

The pressure drop curve of the gas−liquid−solid conical fluidized bed (Figure 2B) is quite different from that of the liquid−solid conical bed. The pressure drop hysteresis disappeared with the gas introduction, likely due to the contribution of bubbles as discussed in previous section. The upward moving

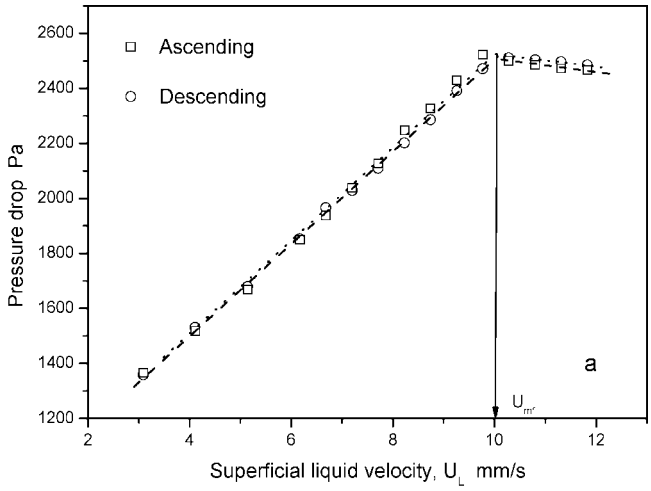

Figure 3. Pressure drop as a function of superficial liquid velocity at inlet of (a) liquid−solid and (b) gas−liquid−solid cylindrical fluidized bed: 0.98 mm GB, 190 mm packed bed height.

bubbles agitated particles to make them loosen up, thus reducing the contact stress between particles in the liquid ascending process (Figures 2B and 3B).

Partial Fluidization. Partial fluidization in the gas−liquid−solid fluidized bed was reached in the same way as in the liquid−solid and gas−solid fluidized beds when the lower region of the bed is fluidized, which corresponds to the maximum pressure drop in the pressure drop vs velocity plot. The minimum partial fluidization velocity can also be determined based on the plot of pressure drop measured over the lower region of the conical bed vs the liquid velocity. The minimum fluidization velocity values for both partial fluidization and full fluidization are plotted in Figure 4. It is seen that the partial fluidization velocity is generally lower than the full fluidization velocity, but the difference becomes smaller as the superficial gas velocity increases.

Minimum Fluidization Velocity and Its Prediction

Experimental data of minimum fluidization velocity in the cylindrical and conical fluidized bed under both liquid−solid and gas−liquid−solid fluidized conditions were obtained based on the pressure drop vs the superficial velocity curve, as illustrated in Figures 2 and 3. For the liquid−solid cylindrical bed, the experimental data were compared with the Ergun equation. The data from the liquid−solid conical fluidized bed

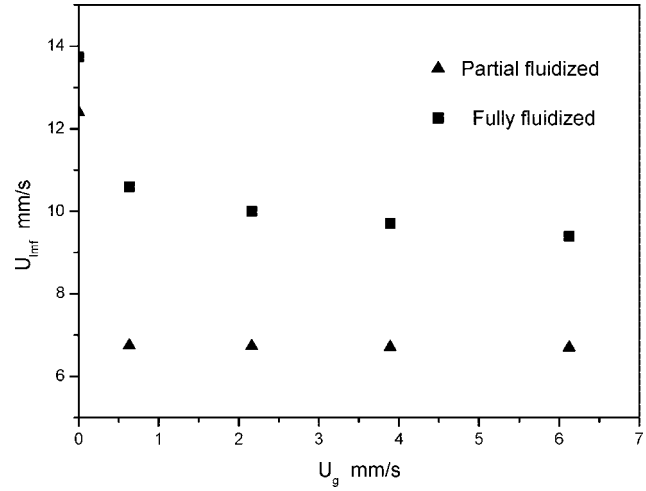

Figure 4. Effect of gas flow rate on the minimum partial fluidization velocity and minimum fluidization velocity.

Table 2. Operating Conditions of the Fluidized Beds

	H m	U_g mm/s	D_1 m	D_0 m
conical bed				
activated carbon	0.115	0, 0.64, 1.67 2.90, 3.89	0.105	0.089
	0.150		0.110	
	0.190		0.115	
0.62 mm GB	0.115	0, 0.64, 3.89, 6.13, 8.47, 11.07	0.105	0.089
	0.150		0.110	
	0.190		0.115	
0.98 mm GB	0.115	0, 0.64, 2.16, 3.89, 6.13	0.105	0.089
	0.150		0.110	
	0.190		0.115	
cylindrical bed				
activated carbon	0.115	0	0.102	0.102
	0.190			
0.62 mm GB	0.115	0	0.102	0.102
	0.190	0, 0.64, 2.16, 3.89, 6.13		
0.98 mm GB	0.115	0	0.102	0.102
	0.190	0, 0.64, 2.16, 3.89, 6.13		

were used to evaluate the equation of Peng and Fan.[13] For gas−liquid−solid three-phase fluidized beds, the models of Song et al.[19] and Zhang[20,21] were selected to predict the minimum fluidization velocity in cylindrical beds and were modified to account for the geometrical shape to predict the minimum fluidization velocity in the gas−liquid−solid conical fluidized bed. The operating conditions of the experiments are listed in Table 2.

Liquid−Solid Fluidized Bed. The Ergun equation[22] is a semiempirical correlation derived by Ergun in 1952 for the frictional pressure loss in a packed column as a function of the Reynolds number:

$$f(u) = C_1 U_l + C_2 U_l^2 \tag{5}$$

Where

$$C_1 = 150\frac{(1-\varepsilon_{mf})^2}{\varepsilon_{mf}^3}\frac{\mu}{(\phi d_p)^2} \tag{6}$$

and

$$C_2 = 1.75\frac{(1-\varepsilon_{mf})}{\varepsilon_{mf}^3}\frac{\rho_l}{\phi d_p} \tag{7}$$

The frictional force is related to the pressure drop by

$$F_s = (-F_f) = A(-\Delta P_F) = f(u)AH \tag{8}$$

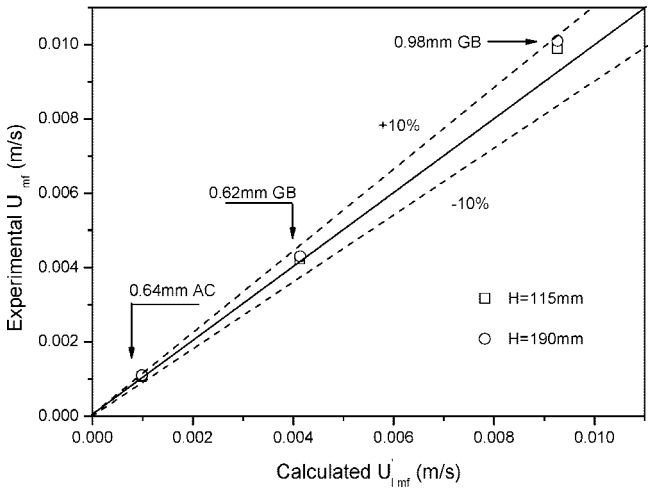

Figure 5. Comparison between the experimentally measured and calculated minimum fluidization velocities of a liquid−solid cylindrical fluidized bed with the Ergun[22] equation for different particles of different bed height.

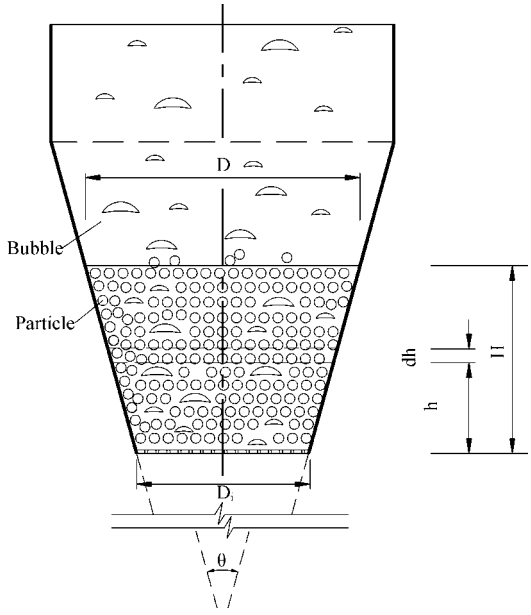

Figure 6. Structure of the conical bed, $\theta = 8°$.

At minimum fluidization conditions, the bed weight is in balance with the frictional force and the net gravitational force

$$F_s + G = 0 \tag{9}$$

While

$$G = -(1 - \varepsilon_{mf})(\rho_s - \rho_l)gAH \tag{10}$$

Substitute eqs 8 and 10 into eq 9, we obtain

$$C_1 U_{lmf} + C_2 U_{lmf}^2 - (1 - \varepsilon_{mf})(\rho_s - \rho_l)g = 0 \tag{11}$$

Equation 11 was used to predict the minimum fluidization velocity for the liquid−solid cylindrical fluidized bed by assuming that the voidage at incipient fluidization was the same as the packed voidage given in Table 1. Figure 5 shows that there is a good agreement between the Ergun equation and our experimental data for the liquid−solids cylindrical fluidized bed.

For a tapered fluidized bed (see Figure 6), the frictional loss will vary with the height because the superficial liquid velocity changes with the height. In a conical bed, for a differential height of dh over which the pressure gradient attributable to the frictional pressure loss can be written as

$$-\frac{dP_F}{dh} = f(u) \tag{12}$$

Here

$$dF_s = (-dF_f) = A(-dP_F) \tag{13}$$

From eqs 5 and 12, one can derive

$$dF_s = A(C_1 U_l + C_2 U_l 2)\, dh \tag{14}$$

Integration of eq 14 over the height

$$F_s = \int_0^{F_s} dF_s = \int_{H_0}^{H_0+H} A(C_1 U_l + C_2 U_l^2)\, dh \tag{15}$$

where

$$A = \frac{1}{4}\pi D^2 \tag{16}$$

$$\frac{D - D_i}{h} = \frac{D_b - D_i}{H} \tag{17}$$

and

$$U_l = \frac{D_b^2}{D^2} U_{li} \tag{18}$$

After integration, we get

$$F_s = \frac{1}{4}\pi D_i^2 H\left[C_1 U_{li} + C_2\left(\frac{D_i}{D_b}\right)U_{li}^2\right] \tag{19}$$

Since

$$dG = -[(1 - \varepsilon_{mf})(\rho_s - \rho_l)]gA\, dh \tag{20}$$

Integration of eq 20 over the bed height

$$G = -\int_0^H dG = -\frac{1}{3}\frac{\pi}{4} D_i^2 H(1 - \varepsilon_{mf})(\rho_s - \rho_l)g\left[\left(\frac{D_b}{D_i}\right)^2 + \frac{D_b}{D_i} + 1\right] \tag{21}$$

At the minimum fluidization condition, $F_s + G = 0$. Combining eqs 9, 19, and 21, one can derive[13,26]

$$\left[C_1 U_{lmf} + C_2\left(\frac{D_i}{D_b}\right)U_{lmf}^2\right] - \frac{1}{3}(1 - \varepsilon_{mf})(\rho_s - \rho_l)g\left[\left(\frac{D_b}{D_i}\right)^2 + \frac{D_b}{D_i} + 1\right] = 0 \tag{22}$$

The minimum fluidization velocity for liquid−solids conical fluidized bed is estimated by eq 22 and compared with current experimental data in Figure 7. It is seen that eq 22 appears to give a reasonable agreement with the experimental data of different particle properties and static bed heights.

Gas−Liquid−Solid Fluidized Bed. To predict the minimum fluidization velocity in three-phase fluidized beds, two semiempirical models are selected for evaluation because both models had been shown to give good agreement with experimental data in the literature.[19–21]

The first model to be examined in this study was developed by Chern et al.[23] and Song et al.[19] In their model, it was assumed that (1) both the gas and liquid flows were one-dimensional, (2) the solid particles were completely wetted by the liquid, and (3) there was no direct contact between the gas and solid. The system can thus be treated as if the gas phase is in the core region, the solid phase is in the wall region, and the liquid phase is between the core and wall regions. On the basis of these assumptions, the total pressure drop could be expressed as[23]

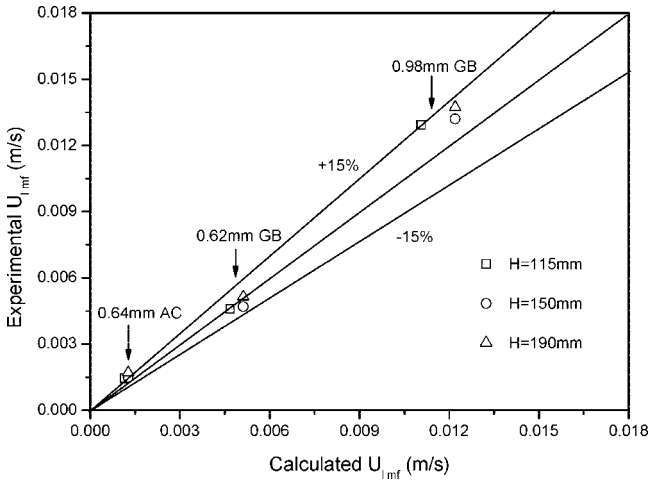

Figure 7. Comparison between the experimentally measured and calculated minimum fluidization velocities with eq 22 for a liquid−solid conical fluidized bed for different particles at different bed heights.

$$(-\Delta P_T) = [(1-\alpha)\rho_l + \alpha\rho_g]gh + (1-\alpha)(-\Delta P_F) \quad (23)$$

This equation relates the total pressure drop $(-\Delta P_T)$ to the frictional pressure loss between the liquid and solid phases, $(-\Delta P_F)$.

In the model of Chern et al.,[23] the frictional pressure loss was expressed in terms of a friction factor, f_c, and $f(u)$ was expressed as

$$f(u) = 4f_c\left(\frac{1}{D_e}\right)\left[\frac{1}{2}\rho_l\left(\frac{U_l}{(1-\alpha)\varepsilon}\right)^2\right] \quad (24)$$

where D_e is defined as an effective diameter of channel for liquid flow. For the separate flow model, it can be derived as

$$D_e = \frac{2(1-\varepsilon_s)}{3\varepsilon_s}[1-\sqrt{\alpha}]\phi d_p \quad (25)$$

By assuming that particles are totally wetted by liquid and that the gas phase has no direct contact with particles, the friction only occurs between the solid phase and the liquid phase. The friction factor, f_c, is thus equal to the friction factor in the liquid−solid fluidized bed and can be calculated by the Ergun[22] equation

$$f_{l-s} = 0.583 + \frac{33.3}{Re_l'} \quad (26)$$

with

$$Re_l' = \frac{D_e\rho_l U_l}{\mu_l \varepsilon_l} \quad (27)$$

The following empirical equations were also suggested by Song et al.[19] for the estimation of the parameter, α, in a fixed bed in eq 25,

$$\alpha = \begin{cases} 0.531 U_l^{-0.350} U_g^{0.977} & (d_p > 3 \text{ mm}) \\ 1.69 U_l^{-0.0902} U_g^{0.955} & (d_p \le 3 \text{ mm}) \end{cases} \quad (28)$$

Total pressure drop, $(-\Delta P_T)$, at minimum fluidization is in balance with the total bed weight and is calculated by

$$(-\Delta P_T) = (\varepsilon_l\rho_l + \varepsilon_s\rho_s + \varepsilon_g\rho_g)gh \quad (29)$$

Combining eq 29 with eqs 23 and 24, one can obtain the following equation for the minimum liquid fluidization velocity for a cylindrical three-phase fluidized bed,

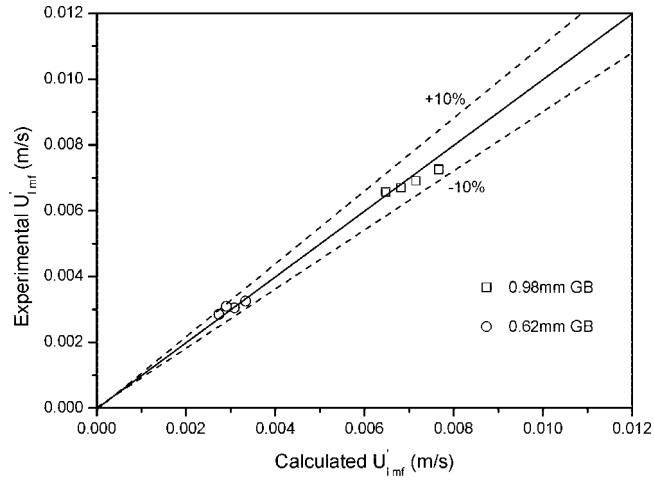

Figure 8. Comparison between the experimentally measured and calculated minimum fluidization velocities using the Song et al. model for gas−liquid−solid cylindrical fluidized bed of different particles.

$$(1-\alpha_{mf})\left\{4f_{l-s}\left(\frac{1}{D_e}\right)\left[\frac{1}{2}\rho_l\left(\frac{U_{lmf}}{(1-\alpha_{mf})\varepsilon_{mf}}\right)^2\right]\right\} + (1-\alpha_{mf})\rho_l g = [(1-\alpha_{mf})\varepsilon_{mf}\rho_l + (1-\varepsilon_{mf})\rho_s]g \quad (30)$$

Note that the above equation assumes that the gas density is negligibly small compared to liquid and particle densities. α_{mf} was calculated with eq 28 in which U_l was set to be equal to U_{lmf} at minmum fluidized conditions.

The bed voidage at minimum fluidization, ε_{mf}, can be estimated by the equations of Wen and Yu[24]

$$\frac{1-\varepsilon_{mf}}{\varepsilon_{mf}^3\phi^2} = 11 \quad (31)$$

and

$$\frac{1}{\phi\varepsilon_{mf}^3} = 14 \quad (32)$$

Figure 8 shows a comparison of the Song et al. model with the minimum fluidization velocity data obtained in the three-phase cylindrical fluidized bed in the current study. Good agreement is observed between the model prediction and the experimental data.

The second model to be examined is the gas-perturbed liquid model proposed by Zhang et al.,[20,21] which assumes that particles are fully supported by the liquid, with the role of the gas being simply to occupy space, thereby increasing the effective velocity of the liquid. This model, applied to three-phase fluidized beds involving Newtonian liquids, equates the liquid-buoyed weight of solids per unit bed volume to the frictional pressure gradient given by Ergun[22] equation applied to the liquid−solids part of the incipiently fluidized bed. The following equation is then derived[20]

$$Re_{lmf} = \sqrt{[150(1-\varepsilon_{mf})/3.5\phi]^2 + \varepsilon_{mf}^3(1-\alpha)^3 Ar/1.75_l} - 150(1-\varepsilon_{mf})/3.5\phi \quad (33)$$

By means of the two approximations by eqs 31 and 32 relating the minimum fluidization voidage, ε_{mf}, to the sphericity with $\phi = 1$, eq 33 can be further simplified to

$$Re_{lmf} = \sqrt{33.7^2 + 0.0406 Ar_l(1-\alpha_{mf})^3} - 33.7 \quad (34)$$

with

$$Re_{lmf} = \frac{\rho_l d_p U_{lmf}}{\mu_l} \quad (35)$$

and

$$Ar_l = \frac{\rho_l(\rho_s - \rho_l) g d_p^{\,3}}{\mu_l^{\,2}} \quad (36)$$

Here α_{mf} is the gas hold-up divided by the total fluid (gas + liquid) hold-up at minimum fluidization, and an empirical equation of Yang et al.[25] shown below was used by Zhang et al.,[20]

$$\alpha_{mf} = \frac{0.16 U_g}{\varepsilon_{mf}(U_g + U_{lmf})} \quad (37)$$

applicable to

$$x = U_g/(U_g + U_l) \le 0.93 \quad (38)$$

Figure 9a compares the minimum liquid fluidization velocity predicted by eqs 34 and 37 with the experimental data for two types of glass beads particles in the cylindrical fluidized bed. The gas perturbed model appears to underestimate the experimental data. One of the possible reasons is that the gas-perturbed model, which was validated with particles of 3.5−6 mm in size by Zhang et al.,[20] may not be very suitable for the fluidized beds with sub-millimeter size particles used in this study due to the relatively large forces imposed by the bubbles on small particles.

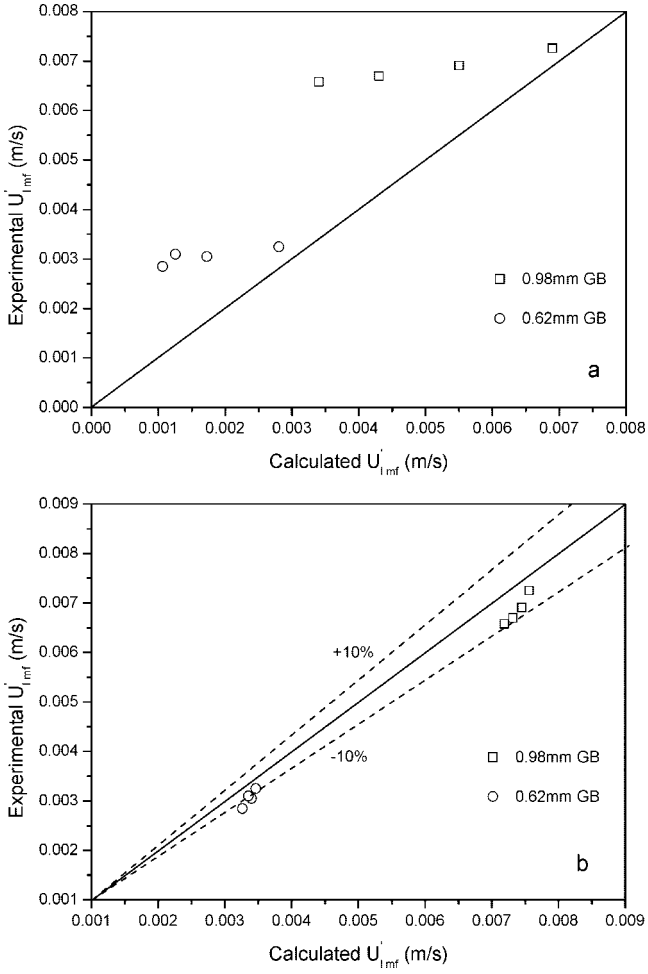

Figure 9. Comparison between the experimentally measured and calculated minimum fluidization velocities using the Zhang et al.[20] model for gas−liquid−solid cylindrical fluidized bed for different particles with α_{mf} from (a) Yang et al.[25] and (b) Song et al.[19]

Furthermore, although the x values ranged from 0 to 0.8 from the current experiment, satisfying the applicable range of eq 37, a close examination reveals that U_{lmf} in eq 34 is very sensitive to α_{mf}. When eq 28 from Song et al. is used to estimate α_{mf} by setting $U_l = U_{lmf}$, it is shown in Figure 9b that the minimum fluidization velocity predicted from eq 34 can give a better agreement with the experimental data, implying that the gas perturbed model can give reasonable agreement with the experimental data obtained from the current three-phase system if the α_{mf} value can be accurately estimated.

To apply the Chern et al.[23] and Song et al.[19] model to three-phase conical beds, the geometrical variation of the column needs to be incorporated. Consider a differential height of dh in the fluidized bed; the drag force on the particles of the particle layer, dF_s, is identical in the magnitude to the frictional force exerted by the fluidizing fluid, dF_s, on the opposite direction. At the minimum fluidization with a fluidized bed height of H, we have

$$F_s = \int_0^H \mathrm{d}F_s = -G = -\int_0^H \mathrm{d}G \quad (39)$$

From eqs 8 and 20,

$$\mathrm{d}F_s = 4 f_{l-s}\left(\frac{1}{D_e}\right)\left[\frac{1}{2}\rho_l\left(\frac{U_l}{(1-\alpha)\varepsilon}\right)^2\right] A\ \mathrm{d}h \quad (40)$$

Combining eq 40 with eqs 16, 18, 26, and 27, one can obtain

$$\mathrm{d}F_s = \frac{\pi}{4}\frac{1.166}{D_e}\frac{D_i \rho_l}{\mathrm{D}^2(1-\alpha)^2\varepsilon^2}U_{li}^{\,2} + \frac{\pi}{4}\frac{66.6}{D_e^{\,2}}\frac{D_i^{\,2}\mu_l}{(1-\alpha)\varepsilon}U_{li} \quad (41)$$

By assuming that the dispersion of the liquid phase and gas phase is uniform in the conical bed and the fraction of gas holdup over total fluid volume fraction is uniform along the bed height, α will remain as a constant along the bed height and can be estimated by eq 28. For the same reason, the equivalent diameter of the conical bed as predicted by eq 25 will remain constant along the bed height.

By substituting eq 17 into eq 41 and integrating over the height, we obtain

$$F_s = \int_0^H \mathrm{d}F_s = \frac{\pi}{4}\frac{1.166}{D_e}\frac{\mathrm{D}_i^{\,3}\rho_l}{D_b(1-\alpha)^2\varepsilon^2}U_{li}^{\,2}H + \frac{\pi}{4}\frac{1.166}{D_e^{\,2}}\frac{D_i^{\,2}\mu_l}{(1-\alpha)\varepsilon}U_{li}H \quad (42)$$

At the minimum fluidization condition, the total frictional force [eq 42] will be equal to the total effective gravity force. In view that the air density is much lower than the water and particle densities, the buoyancy contribution from the gas can be neglected. Thus, the effective gravity force still can be expressed by eq 21, with ε_{mf} being equal to the sum of gas and liquid voidage fractions at the minimum fluidized condition. One obtains

$$\frac{1.166}{D_{emf}}\frac{D_i}{D_b}\frac{\rho_l}{(1-\alpha_{mf})^2\varepsilon_{mf}^{\,2}}U_{lmf}^{\,2} + \frac{1.166}{D_{emf}^{\,2}}\frac{\mu_l}{(1-\alpha_{mf})\varepsilon_{mf}}U_{lmf} - \frac{1}{3}HD_i^{\,2}\left\{\frac{\pi}{4}(1-\varepsilon_{mf})(\rho_s-\rho_l)\left[\left(\frac{D_b}{D_i}\right)^2 + \frac{D_b}{D_i} + 1\right]g\right\} = 0 \quad (43)$$

where ε_{mf} can be calculated by eqs 31 and 32.

To apply the gas-perturbed model of Zhang et al.[20] to the three-phase conical fluidized bed, the following equation can be derived for the minimum liquid fluidization velocity in the

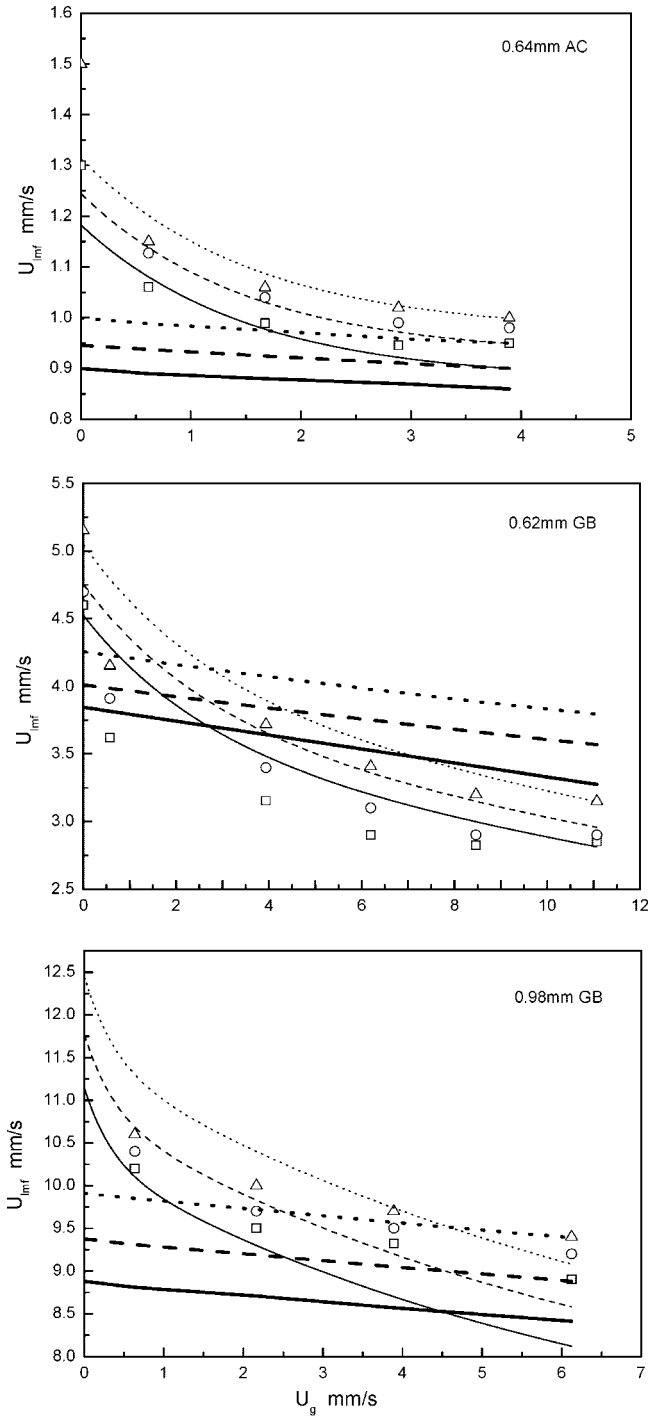

Figure 10. Comparison of minimum fluidization velocity data obtained in the conical gas−liquid−solid fluidized bed at different bed height with predictions from the Song et al.[19] (thin lines) and Zhang et al.[20] models (thick lines).

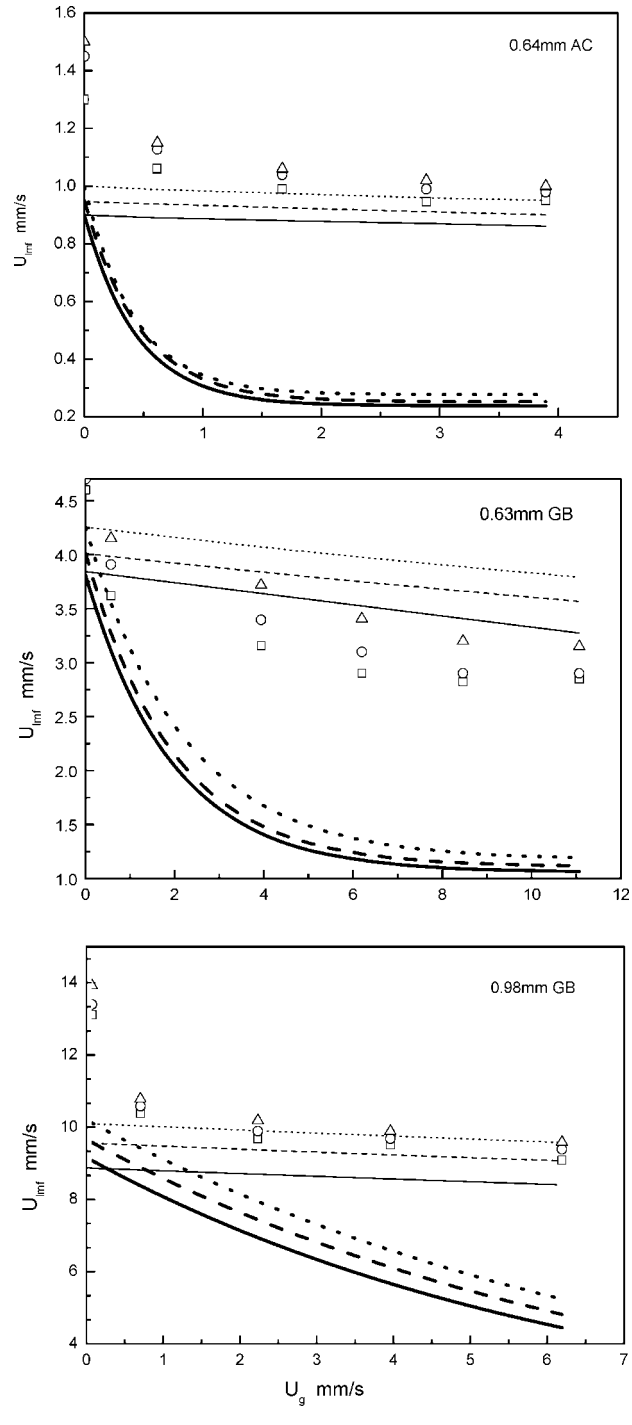

Figure 11. Comparison of minimum fluidization velocity data with predictions of Zhang et al.[20] model with α_{mf} value estimated from the Yang et al.[25] (thick lines) and the Song et al.[19] (thin lines) correlations.

three-phase conical fluidized bed following the same procedures as for the liquid−solid conical fluidized bed,

$$(Re_i)_{lmf} = [\sqrt{33.7^2 + 0.0406 Ar_l (1-\alpha_{mf})^3 K_1 K_2} - 33.7]/K_2 \quad (44)$$

where

$$K_1 = (D_i/D_b)$$

$$K_2 = [(D_b/D_i)^2 + (D_b/D_i) + 1]/3 \quad (45)$$

α_{mf} can be obtained by eqs 28 or 37.

Figure 10 compares the prediction from the modified Song et al. model and the modified Zhang et al.[20] model with the experimental data in the gas−liquid−solid conical fluidized bed. It is seen that, in general, the Song et al. model gives better

agreement with the experimental data for the three types of particles with different static bed height, with the error between calculated and measured minimum velocity values being within 20%.

As in the cylindrical column, we also replaced the Yang et al.[25] equation [eq 37] with the Song et al.[19] equation [eq 28] for the prediction of α_{mf} in the modified Zhang et al.[20] model, in view of the improved prediction in the cylindrical unit before. As shown in Figure 11, the Zhang et al. model gives much better agreement with the experimental data when the Song et al. equation is used for the estimation of the α_{mf} value. Most of the predicted minimum velocities fall within 20% of the error range. The conclusion is that both Song et al. and Zhang et al. models can be used to predict the minimum fluidization velocity in the tapered three-phase fluidized bed if a right value for the gas holdup, α_{mf}, can be obtained.

Conclusions

In a gas−liquid−solid conical fluidized bed, the upward flow of bubbles tends to exert more agitation to packed particles in the upper region of the column, loosening particles to reduce the particle−particle contact. As a result, the pressure drop hysteresis, which is the unique characteristic of a liquid−solid tapered fluidized bed, disappeared in gas−liquid−solid conical fluidized beds at relatively high gas flow rate. The Ergun equation is shown to be capable of predicting the minimum fluidization velocities in liquid−solid cylindrical and conical fluidized beds when the geometrical configuration is taken into consideration. For the three-phase fluidized bed system, the modified model of Song et al.[19] shows better agreement on the minimum fluidization velocity data from this study than the modified Zhang et al.[20] model. However, the prediction from the Zhang et al. model can be improved when α_{mf}, the fractional gas holdup at minimum fluidization, is estimated by the Song et al. equation.

Acknowledgment

The authors are grateful for the financial support from the Natural Science and Engineering Research Council of Canada (NSERC) and the China Scholarship Council (CSC).

Note Added after ASAP Publication: The current affiliation of author Zhou has been updated from the version posted to the Web June 25, 2008. The corrected version was reposted to the Web on November 13, 2008.

Appendix A

Integration of force equations

$$\int_0^H d\mathrm{G} = -\int_0^H [(1-\varepsilon_{mf})(\rho_s-\rho_l)]gA_b\,\mathrm{d}h$$

$$= -\int_0^H [(1-\varepsilon_{mf})(\rho_s-\rho_l)]g\left(\frac{1}{4}\pi D^2\right)\mathrm{d}h$$

$$= -\frac{1}{4}\pi[(1-\varepsilon_{mf})(\rho_s-\rho_l)]g\int_0^H \left(\frac{D_b-D_i}{H}h+D_i\right)^2\mathrm{d}h$$

$$= -\frac{1}{4}\pi[(1-\varepsilon_{mf})(\rho_s-\rho_l)]g\left\{\left(\frac{D_b-D_i}{H}\right)^2\frac{1}{3}h^3\Big|_0^H + \frac{2D_i(D_b-D_i)}{H}\frac{1}{2}h^2\Big|_0^H + D_i^2h\Big|_0^H\right\}$$

$$= -\frac{1}{3}HD_i^2\left\{\frac{\pi}{4}(1-\varepsilon_{mf})(\rho_s-\rho_l)\left[\left(\frac{D_o}{D_i}\right)^2+\frac{D_o}{D_i}+1\right]g\right\}$$

Appendix B

$$\frac{D-D_i}{h}=\frac{D_b-D_i}{H}$$

$$D=\frac{D_b-D_i}{H}h+D_o$$

$$\int_0^H\frac{1}{D^2}=\int_0^H\left(\frac{D_b-D_i}{H}h+D_b\right)^{-2}\mathrm{d}h$$

$$=\int_0^H\frac{\left(\frac{H}{D_b-D_i}\right)^2}{\left(h+\frac{HD_i}{D_b-D_i}\right)^2}\mathrm{d}h$$

$$=\left(\frac{H}{D_b-D_i}\right)^2\int_0^H\left(h+\frac{HD_i}{D_b-D_i}\right)^{-2}\mathrm{d}\left(h+\frac{HD_i}{D_b-D_i}\right)$$

$$=-\left(\frac{H}{D_b-D_i}\right)^2\left(h+\frac{HD_i}{D_b-D_i}\right)^{-1}\Big|_0^H$$

$$=\frac{H}{D_iD_b}$$

Notations

$(-\Delta P_T)$ = total pressure drop, N/m^2
$(-\Delta P_F)$ = pressure drop due to frictional loss, N/m^2
A = cross-sectional area of cylindrical bed or of conical bed at the height of h, m^2
Ar_l = liquid phase Archimedes number, defined by eq 36
C_1, C_2 = constant in the Ergun equation defined by eqs 6 and 7
D_i = diameter of conical bed at the entrance, m
D_b = diameter of conical bed at the upper bed surface, m
D = diameter of conical bed at the height of h, m
D_e = equivalent diameter, defined by eq 25, m
D_{emf} = equivalent diameter at minimum fluidization conditions, m
d_p = particle diameter, m
F_f = frictional force exert on fluid, N
F_s = frictional force exert on particles, N
f_c = modified friction factor in three-phase bed defined by eq 24
f_{l-s} = modified friction factor in liquid−solid bed defined by eq 26
G = effective weight of the particles, N
g = gravitational acceleration, m/s^2
H = toal expanded bed height, m
h = vertical distance above the distributor, m
Re' = liquid Reynolds number based on linear liquid velocity, defined by eq 27
Re_{lmf} = liquid Reynolds number at minimum fluidization velocity, defined by eq 35
U_g = superficial gas velocity of cylindrical fluidized bed or of conical bed at the entrance, m/s
U_l = superficial liquid velocity of cylindrical bed or of conical bed at the height of h, m/s
U_{li} = superficial liquid velocity at the entrance, m/s
U_{lmf} = minimum fluidization liquid velocity of cylindrical fluidized bed or of conical bed at the entrance, m/s
W = weight of dry particles, kg

Greek Letters

α = fractional gas holdup over total fluid volume fraction, $= \varepsilon_g/(\varepsilon_g+\varepsilon_l)$
α_{mf} = fractional gas holdup over total fluid volume fraction at minimum fluidization condition

ε = voidage of fluidized bed
ε_0 = voidage of the fixed bed
ε_{mf} = voidage at minimum fluidization
ε_p = porosity of particles
ε_s = solids holdup
ρ_l = liquid density, kg/m^3
ρ_r = skeleton density, kg/m^3
ρ_s = solid (particle) density, kg/m^3
ρ_w = wet density of porous particle, kg/m^3
μ_l = fluid viscosity, N$_s$/m^2
Φ = sphericity of the solid particle

Literature Cited

(1) Davidson, J. F.; Clift, R.; Harrison, D. *Fluidization*, 2nd ed.; Academic Press: London, Toronto, 1985.

(2) Geldart, D. *Gas Fluidization Technology*; Wiley & Sons: Chichester, 1986.

(3) Kunii, D.; Levenspiel, O. *Fluidization Engineering*, 2nd ed.; Butterworth-Heinemann: Boston, 1991.

(4) Kwauk, M. *Fluidization: Idealized and Bubbleless, with Applications*; Science Press: Beijing; Ellis Horwood: New York, Toronto, 1992.

(5) Crowe, C. T. *Multiphase flow handbook*; Taylor & Francis Group: LLC: London, 2006.

(6) Fan, L.-S.; Fu, J. K.; Long, T. R.; Tang, W.-T. Characteristics of Draft Tube Gas-Liquid Solid Fluidized-Bed Bioreactor with Immobilized Living Cells for Phenol Degradation. *Biotechnol. Bioeng.* **1987**, *30* (4), 498.

(7) Hirata, A.; Meutia, A. A.; Osawa, M.; Arai, M. Effect of Oxygen Supply Condition and Specific Biofilm Interfacial Area on Phenol Removal Rate in a Three-Phase Fluidized Bed Bioreactor. *Can. J. Chem. Eng.* **2000**, *78*, 95.

(8) Inguanzo, M.; Dominguez, A.; Mendez, J. A.; Blanco, C. G.; Pis, J. J. On the Pyrolysis of Sewage Sludge: the Influence of Pyrolysis Conditions on Solid, Liquid and Gas Fractions. *J. Anal. Appl. Pyrol.* **2002**, *63* (1), 209.

(9) Zhang, J.; Jiang, F.-L.; Yang, Y.-D.; Li, J.-P. Catalyst-Assisted Vapor-Liquid-Solid Growth of Single-Crystal Ca $_2$O$_3$ Nanobelts. *J. Phys. Chem. B.* **2005**, *109* (27), 13143.

(10) Toyohara, H.; Kawamura, Y. Fluidization of a Tapered Fluidized-Bed of a Binary Particle-Mixture. *Int. Chem. Eng.* **1992**, *33*, 164.

(11) Webster, G. H.; Perona, J. The Effect of Taper Angle on the Hydrodynamics of a Tapered Liquid-Solid Fluidized Bed. *A.I.Ch.E. Syrup.* **1990**, *86*, 104.

(12) Wu, C. S.; Huang, J. S. Expansion Characteristics of Tapered Fluidized-Bed Bioreactors. *Advances in Bioprocess Engineering*; Galindo, E., Ramirez, O. T., Ed.; Kluwer Academic: Netherlands. 1998; p 355.

(13) Peng, Y.; Fan, L. T. Hydrodynamic Characteristics of Fluidization in Jiquid-Solid Tapered Beds. *Chem. Eng. Sci.* **1997**, *52* (14), 2277.

(14) Jing, S.; Hu, Q.; Wang, J.; Jin, Y. Fluidization of Coarse Particles in Gas-Solid Conical Bed. *Chem. Eng. Process.* **2000**, *39*, 379.

(15) Schaafsma, S. H.; Marx, T.; Hoffmann, A. C. Investigation of the Particle Flowpattern and Segregation in Tapered Fluidized Bed Granulators. *Chem. Eng. Sci.* **2006**, *61*, 4467.

(16) Shi, Y.; Yu, Y. S.; Fan, L. T. Incipient Fluidization Condition for a Tapered Fluidized Bed. *Ind. Eng. Chem. Fundam.* **1984**, *23*, 484.

(17) Venkatesh, R. D.; Chaouki, J.; Klvana, D. Fluidization of Cryogels in a Conical Column. *Powder Tech.* **1996**, *89*, 179.

(18) Legros, R.; Charbonneau, S.; Mayer, C. R. *Engineering Fluidization, Fluidization (VIII)*; New York, 1996; p 639.

(19) Song, G.-H.; Bavarian, F.; Fan, L.-S. Hydrodynamics of Three-Phase Fluidized Bed Containing Cylindrical Hydrotreating Catalysts. *Can. J. Chem. Eng.* **1989**, *67*, 265.

(20) Zhang, J.-P.; Epstein, N.; Grace, J. R. Minimum Fluidization Velocityes for Gas-Liquid-Solid Three-Phase System. *Power Tech.* **1998**, *100*, 113.

(21) Zhang, J.-P. Bubble Columns and Three-Phase Fluidized Beds: Flow Regimes and Bubble Characteristics. Dr. thesis, 1996.

(22) Ergun, S. *Chem. Eng. Prog.* **1952**, *48*, 89.

(23) Chern, S.-H.; Muroyama, K.; Fan, L.-S. Hydrodynamics of Constrained Inverse Fluidization and Semifluidization in a Gas-Liquid-Solid System. *Chem. Eng. Sci.* **1983**, *38*, 1167.

(24) Wen, C. Y.; Yu, Y. H. Mechanics of Fluidization. *Chem. Eng. Prog. Symp. Ser.* **1966**, *62*, 100.

(25) Yang, X. L.; Wild, G.; Euzen, P. Study of Liquid Retention in Fixed-Bed Reactors with Upward Flow of Gas and Liquid. *Int. Chem. Eng.* **1993**, *33*, 72.

(26) Bi, H. T.; Macchi, A.; Chaouki, J.; Legros, R. Minimum Spouting Velocity of Conical Spouted Beds. *Can. J. Chem. Eng.* **1997**, *75*, 460.

Received for review February 1, 2008
Revised manuscript received April 15, 2008
Accepted April 16, 2008

IE8001974